JOC The Journal of Organic Chemistry

Article

pubs.acs.org/joc

Phenyl-imidazolo-cytidine Analogues: Structure–Photophysical Activity Relationship and Ability To Detect Single DNA Mismatch

Marina Kovaliov, Michal Weitman, Dan Thomas Major, and Bilha Fischer*

Department of Chemistry, Gonda-Goldschmied Medical Research Center and the Lise-Meitner-Minerva Center of Computational Quantum Chemistry, Bar-Ilan University, Ramat-Gan 52900, Israel

Supporting Information

ABSTRACT: To expand the arsenal of fluorescent cytidine analogues for the detection of genetic material, we synthesized *para*-substituted phenyl-imidazolo-cytidine (^{Ph}ImC) analogues **5a–g** and established a relationship between their structure and fluorescence properties. These analogues were more emissive than cytidine (λ_{em} 398–420 nm, Φ 0.009–0.687), and excellent correlation was found between Φ of **5a–g** and σ_p^- of the substituent on the phenyl-imidazolo moiety (R^2 = 0.94). Calculations suggested that the dominant tautomer of ^{Ph}ImC in methanol solution is identical to that of cytidine. DFT calculations of the stable tautomer of selected ^{Ph}ImC analogues suggested a relationship between the HOMO–LUMO gap and Φ and explained the loss of fluorescence in the nitro analogue. Incorporation of the CF_3-^{Ph}ImdC analogue into a DNA probe resulted in 6-fold fluorescence quenching of the former. A *17-fold* reduction of fluorescence was observed for the *G-matched* duplex vs **ODN(CF_3-^{Ph}ImdC)**, while for *A-mismatched* duplex, only a *2-fold* decrease was observed. Furthermore, since the quantum yield of **ODN(CF_3-^{Ph}ImdC):ODN(G)** was reduced 17-fold vs that of a single strand, whereas that of **ODN(CF_3-^{Ph}ImdC):ORN(G)** was reduced only 3.8-fold, **ODN(CF_3-^{Ph}ImdC)** appears to be a DNA-selective probe. We conclude that the **ODN(CF_3-^{Ph}ImdC)** probe, exhibiting emission sensitivity upon single nucleotide replacement, may be potentially useful for DNA single nucleotide polymorphism (SNP) typing.

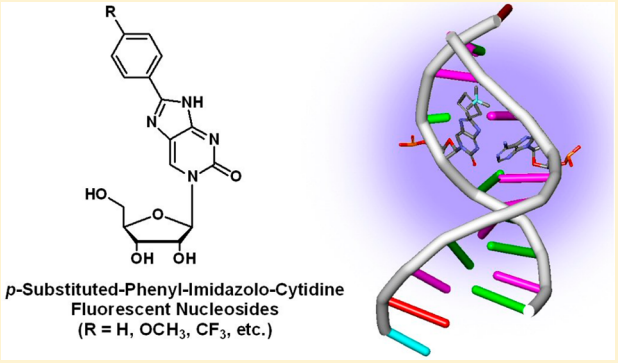

INTRODUCTION

Fluorescence-based methods have been instrumental in advancing biophysical assays and high throughput screening techniques, particularly for identification and quantification of nucleic acids.[1−4] For the latter application, nucleic acids are not useful, as native nucleobases are practically nonemissive.[5−7] Hence, conjugation of oligonucleotide probes with various dye molecules has become a common procedure. However, most dye molecules are large and hydrophobic and have limited water solubility. Furthermore, a large dye molecule attached to a nucleotide alters the efficiency of enzymatic incorporation into DNA/RNA, resulting in different levels of labeling and prohibits quantification of nucleic acids. End labeling with common fluorescent tags (e.g., cyanine dyes) is synthetically simple yet is far from being optimal since end labels are not necessarily sensitive to remote binding events and such fluorophores are large, charged, and frequently noninnocent.[8] Currently, there is a great need for new, improved fluorescent nucleoside analogues with minimal structural perturbation yet with high quantum yields and relatively long emission wavelength.

Over the past decade, a number of intrinsically fluorescent nucleoside analogues that can replace natural DNA bases as oligonucleotide probes have been reported as alternatives to dye-substituted nucleosides.[9−11] Thus, the fluorescent properties of the natural nucleosides were significantly improved by extending the purine/pyrimidine π-system.[1−4,12−18] Several fluorescent pyrimidine analogues with extended fluorophores have been reported (Figure 1). For example, imidazolo-cytidine, **1**, exhibited a longer emission wavelength and higher quantum yield as compared to cytidine (λ_{em} 390 nm; Φ 0.051 vs λ_{em} 303 nm; Φ 0.00008).[19] Emission properties of compound **1** enabled studies on permeation and inhibition of human nucleoside transporters.[20−22]

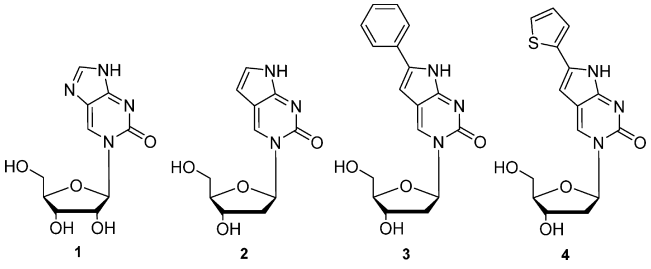

Figure 1. Fluorescent fused-cytidine (C) and 2′-deoxycytidine (dC) nucleoside analogues: imidazolo-C analogue, **1**; pyrrolo-dC, **2**; phenylpyrrolo-dC, **3**; thiophene-yl-pyrrolo-dC, **4**.

Received: May 29, 2014
Published: July 3, 2014

Pyrrolo-2′-deoxycytidine, **2** (λ_{abs} 353 nm, λ_{em} 448 nm, Φ 0.038 in Tris buffer) and phenyl-pyrrolo-2′-deoxycytidine, **3** (λ_{abs} 360 nm, λ_{em} 465 nm, Φ 0.31 in phosphate buffer), have found use as fluorimetric reporting groups.[23] The substitution of the phenyl group on the pyrrole ring not only yielded a much more emissive compound but also contributed to the stabilization of the duplexes.[11,24,25] Pyrrolo-2′-deoxycytidine was also extended via conjugation to a thiophene ring, **4**, resulting in improved fluorescence properties (λ_{abs} 369 nm, λ_{em} 469 nm, Φ 0.41 in H_2O).[26]

Recently, we have reported on new fluorescent pyrimidine nucleosides, phenyl-imidazolo-cytidine analogues (^{Ph}ImC) **5a–d**, based on fusion of the imidazolo moiety to cytidine and further conjugation of the *para*-phenyl substituted ring (Figure 2).[27] These compounds fluoresce in the blue region and exhibit quantum yields and maximum emission that are 7000-fold larger and ca. 110 nm red-shifted vs that of cytidine.

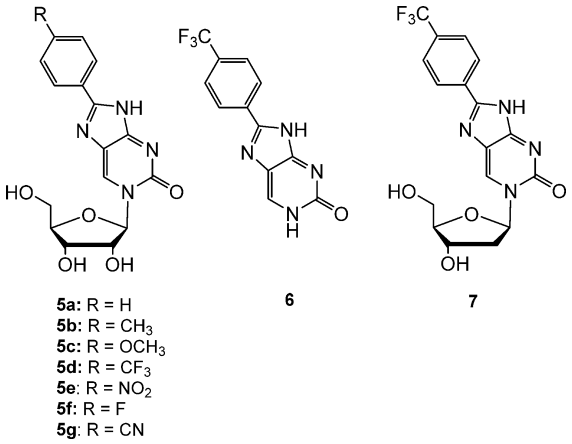

Figure 2. Phenyl-imidazolo-cytosine analogues studied here.

These fluorescent nucleoside derivatives have been well characterized and an effect of the phenyl ring substituent on fluorescence properties of the parent compound was observed (e.g., **5d**; λ_{abs} 346 nm; λ_{em} 411 nm; Φ 0.617 vs **5a**; λ_{abs} 342 nm; λ_{em} 402 nm; Φ 0.198 in MeOH), but no clear dependence of their fluorescence on the electronic character of the substituent was established. These data led us to extend our research on structure–activity relationship of the imidazolo-cytidine series.

Although there are numerous reports on the structural dependence of fluorescence properties,[28−30] i.e., λ_{em} and Φ values, there are a limited number of reports on the effect of substituents on the fluorescence of nucleoside analogues. Recently, we have explored the relationship between the nature of substituents on cinnamyl moiety in 8-(substituted cinnamyl)adenosine and the fluorescence properties of the latter. We found excellent correlation between λ_{ab} and Φ of the analogues and the computed HOMO and LUMO energy levels of 8-vinyl-9-methyladenine (fluorescent molecule) and substituted toluene rings (fluorescence modulators).[18]

Here, we first targeted the establishment of relationship between the chemical nature of the substituent on the phenyl-imidazolo moiety and the fluorescence characteristics of the resulting imidazolo-cytidine analogues **5a–g**. Next, we selected one of the most promising fluorescent nucleosides, CF_3-^{Ph}ImC, **5d**, and investigated the effect of its incorporation into an oligonucleotide on its photophysical properties.

Specifically, we report on the synthesis and photophysical properties of a series of *para*-substituted-^{Ph}ImC analogues, **5a–g**. We analyzed the relationship between the fluorescence properties of several ^{Ph}ImC analogues and the nature of the substituents as reflected by several Hammet constants. In addition, we analyzed this relationship by density functional theory (DFT) calculations. In particular, we identified the most stable tautomers of the ^{Ph}ImCs, compared their computed and experimental absorption spectra, and correlated the experimental Φ values with the computed HOMO–LUMO gaps. In addition, we synthesized and studied the fluorescent properties of CF_3-^{Ph}Im-cytosine, **6**. Based on the established structure–activity relationship, we synthesized *p*-CF_3-imidazolo-2′-deoxycytidine (CF_3-^{Ph}ImdC), **7**, and incorporated it into DNA. Finally, we evaluated the influence of **7** on duplex stability and its ability for single mismatch detection.

Substituted ^{Ph}ImdC analogues could be used in a wide range of applications, including but not limited to single nucleotide polymorphism (SNP) detection.[31−35] The novel compounds may be employed as useful reporters of sequence and structure of nucleic acids, e.g., the resolution of hybridization events,[36] folding,[37] conformational change,[38] as well as enzyme action.[39] In addition, the novel analogues may be used for microenvironmental probing studies for detection of nucleobase damage,[40] depurination/depyrimidation,[41] and base flipping.[37]

RESULTS AND DISCUSSION

Synthesis of ^{Ph}ImC and Its Derivatives. We have previously reported the synthesis of *para*-substituted ^{Ph}ImC analogues **5a–d**, which exhibited improved photophysical properties as compared to imidazolo-cytidine, **1**.[27] Here, we targeted the synthesis of additional analogues representing a wider chemical space (**5a–g**).

Synthesis of analogues **5a–g** was achieved by condensation of per-benzoylated 5-aminocytidine, **8**,[42,43] with *para*-substituted benzaldehyde **9a–g**, in the presence of *p*-TsOH (20 mol %), in DMF at 80 °C, to give **10a–g** in 36–47% yield.[44] Addition of 1 M NaOH in MeOH, at room temperature for 1 h, yielded **5a–g** in 80–85% yield (Scheme 1).

Scheme 1. Synthesis of ^{Ph}ImC Analogues 5a–g

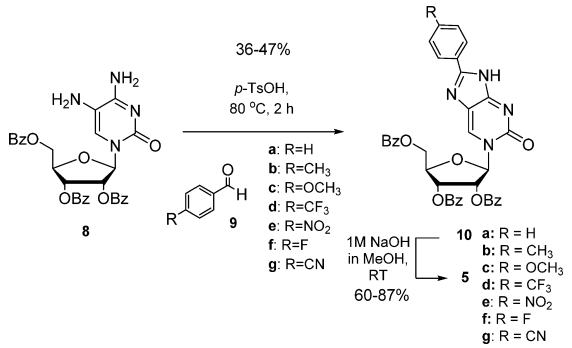

To examine the effect of ribose and 2′-deoxyribose on the photophysical properties of ^{Ph}ImC analogues we synthesized the cytosine analogue, **6**, related to the highly emissive compound **5d** (Scheme 2).[27] 5-Nitrocytosine, **12**, was readily prepared from cytosine **11** in the presence of fuming nitric acid[45] and was then subjected to hydrogenation to provide 5-aminocytosine, **13**.[46] Condensation of **13** with *p*-CF_3-

dx.doi.org/10.1021/jo5011944 | J. Org. Chem. 2014, 79, 7051–7062

Scheme 2. Synthesis of *p*-CF_3-^{Ph}Im-cytosine

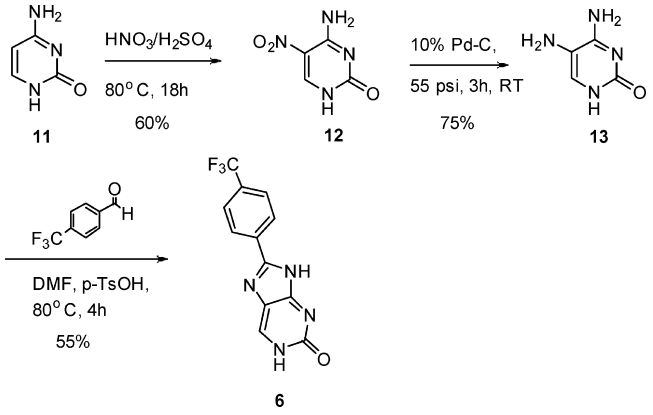

benzaldehyde in the presence of *p*-TsOH afforded compound **6** in 55% yield.

Next, we prepared CF_3-^{Ph}ImdC phosphoramidite, **20**, to be incorporated into an oligonucleotide (Scheme 3). First, 2′-deoxyuridine, **14**, was acetylated and then nitrated with nitrosonium tetrafluoroborate in dimethylformamide to give **15**.[47] Next, compound **15** was transformed into the corresponding cytidine analogue **16** using triisopropylbenzenesulfonyl chloride (TPSCl) followed by treatment with NH_4OH.[48] After hydrogenation of **16**, protected 5-amino-2′-deoxycytidine, **17**, was reacted with *p*-CF_3-benzaldehyde in the presence of *p*-TsOH to afford compound **18** in 50% yield. Deacetylation of **18** with sodium methoxide afforded nucleoside **7** in 80% yield. The corresponding phosphoramidite **20** was obtained in two steps: 5′ protection using 4,4′-dimethoxytrityl chloride in anhydrous pyridine followed by phosphorylation with 2-cyanoethyl *N,N,N′,N′*-tetraisopropylphosphorodiamidite in the presence of tetrazole. This gave, after filtration of diisopropylammonium tetrazolide, a concentrated solution of **20** that was diluted with CH_3CN to a formal concentration of 0.1 M and immediately used for the automated synthesis of the oligonucleotide. This procedure allowed us to carry out the synthesis of the DNA probe without any loss of the phosphoramidite **20** in the purification step.

Absorption and Fluorescence Spectra. The photophysical properties of *para*-substituted ^{Ph}ImC compounds **5a−g** were studied in methanolic solutions. The fluorescence quantum yields were determined using quinine sulfate in 0.1 M H_2SO_4 (λ_{ex} 350 nm, λ_{em} 446 nm, Φ 0.54) as a reference.[49] The concentrations of the samples were in the linear range in which the Beer−Lambert law applies, and the optical density (OD) was less than 0.05 to avoid the inner filter effect.[50] The fluorescent properties of analogues **5a−g** are summarized in Table 1. The absorption spectra, fluorescence intensity, and normalized fluorescence are presented in Figures 3 and 4. The conjugation of the *para*-substituted phenyl ring to the parent imidazolo-cytidine, **1** (λ_{ex} 322 nm, λ_{em} 390 nm, Φ 0.051 in methanol),[20−22] indeed improved the photophysical properties, e.g. **5d** (λ_{ex} 346 nm, λ_{em} 411 nm, Φ 0.617) and **5g** (λ_{ex} 350 nm, λ_{em} 420 nm, Φ 0.687).

The various *p*-substituents in **5a−g** had a minor effect on the wavelength of the absorption maxima, which were in the range of 342−350 nm, except for the $-NO_2$, analogue, **5e** (λ_{ab} 368 nm). The electron-withdrawing substituents evoked more efficiently bathochromic shift compared to electron-donating substituents (e.g., $-NO_2$ analogue, **5e**, vs $-OCH_3$ analogue, **5c**, and the parent compound, **5a**: 368 and 347 vs 342 nm).

Although the absorption maxima were rather insensitive to the alteration of the substituents on the phenyl ring, the emission maxima were more affected by the substituents (Figure 4). The compounds having the largest Stoke's shift are **5d** and **5g** (65 and 70 nm), and the smallest shift was observed for **5e** (30 nm) (Table 1).

The longest λ_{em} was observed for analogue **5g** bearing a −CN group (420 nm). Generally, electron-withdrawing

Scheme 3. Synthesis of CF_3-^{Ph}ImdC Phosphoramidite 20[a]

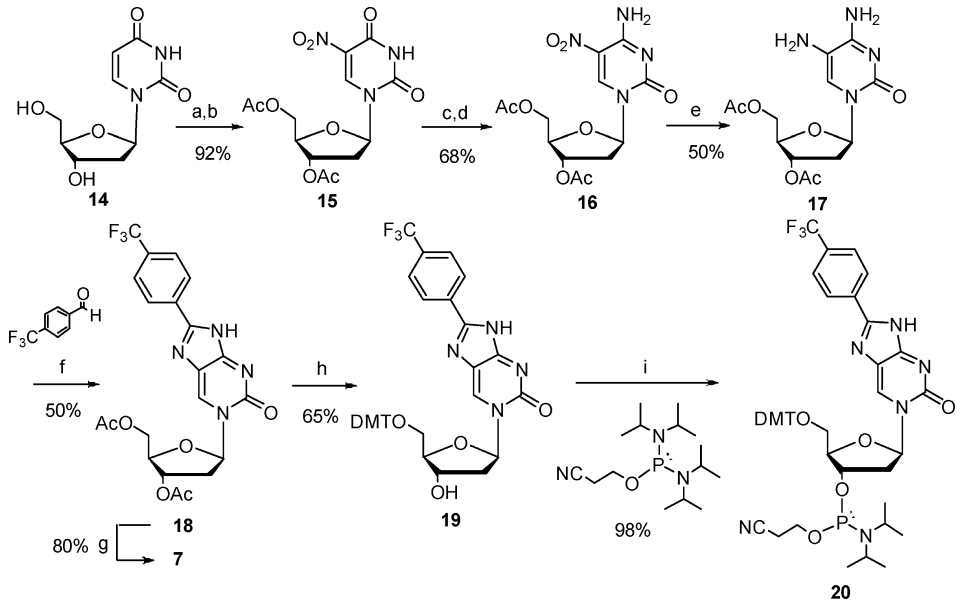

[a]Reaction conditions: (a) Ac_2O in pyridine, overnight, rt; (b) $NOBF_4$ in DMF, 30 min, rt; (c) TPSCl, DMAP, TEA in CH_3CN, 3 h, rt; (d) 33% NH_4OH in CH_3CN, 2 h, rt; (e) 10% Pd/C, 1.5 atm, THF, AcOH, 6 h, rt; (f) *p*-CF_3-benzaldehyde, *p*-TsOH in DMF, 4 h, 80 °C; (g) NaOMe in MeOH, 30 min, rt; (h) DMTCl in pyridine, 2.5 h, rt; (i) *N,N,N′,N′*-tetraisopropylphosphorodiamidite, tetrazole in CH_3CN, 45 min, rt.

dx.doi.org/10.1021/jo5011944 | J. Org. Chem. 2014, 79, 7051−7062

Table 1. σ Values and Photophysical Properties of Analogues 5a–g in MeOH

	R	σ_p[51]	σ_p^+[52]	σ_p^-[53]	λ_{ab} (nm)	λ_{em} (nm)	Stoke's shift (nm)	Φ^a	ε_{max} (cm^{-1} M^{-1})
5a	H	0	0	0	342	402	60	0.215	7400
5b	CH_3	−0.170	−0.311	−0.17	344	403	59	0.198	8800
5c	OCH_3	−0.268	−0.778	−0.26	347	405	58	0.233	9900
5d	CF_3	0.541	0.612	0.65	346	411	65	0.617	11250
5e	NO_2	0.778	0.790	1.27	368	398	30	0.009	13100
5f	F	0.062	−0.073	−0.03	347	404	57	0.312	10540
5g	CN	0.660	0.659	1.00	350	420	70	0.687	14150

[a]Quantum yields were determined using quinine sulfate as a standard.

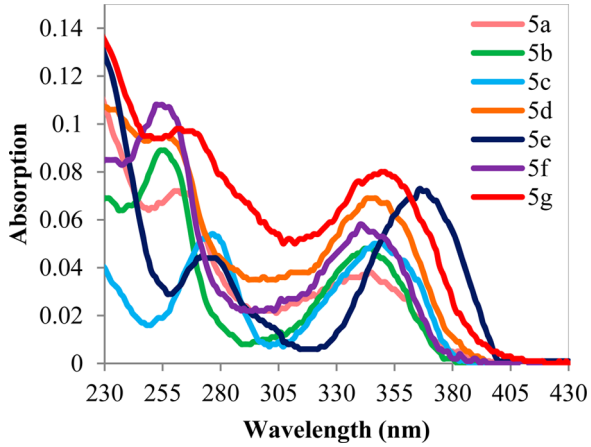

Figure 3. UV–vis spectra of *para*-substituted ^{Ph}ImC analogues in MeOH (5.5 μM).

substituents, e.g., $-CF_3$ and −F, led to a bathochromic shift of the emission maxima (see **5d** and **5f**, Table 1). Analogues **5d** and **5g** bearing a $-CF_3$ or −CN group exhibited the highest quantum yields (0.671 and 0.687, respectively), exceeding also those of the related phenyl-pyrolo-cytidine analogues.[11,25] Although analogue **5e** bears the most electron-withdrawing group, $-NO_2$, in this series of compounds, it was practically nonfluorescent with quantum yield of 0.009. Analogues **5b** and **5c** bearing an electron-donating group, $-CH_3$ or $-OCH_3$, exhibited quantum yields of 0.198 and 0.233, respectively, similar to the parent compound, **5a** (Φ 0.215).

Next, we analyzed the substituent-dependent photophysical properties of analogues **5a–g** by seeking first correlation with various σ values of the substituents. Previous reports indicated a linear correlation between sigma values and fluorescent properties of several organic compounds.[54−56] Thus, we attempted to correlate quantum yields and emission data with the electronic properties of the phenyl-imidazolo- moiety in analogues **5a–g** as reflected by the σ Hammett constant, σ_p, of the phenyl substituents.

The σ constant σ^- is designated in the case where negative charge buildup in the transition state occurs, and the rate of the reaction is consequently accelerated by electron-withdrawing groups.[57] On the other hand, σ^+ constants were developed for substituents conjugated with a reaction center which could effectively delocalize a positive charge. Hence, an electron-donating group will accelerate the rate of the reaction by resonance stabilization.[58] To elucidate the formation of any charge in ^{Ph}ImC system in the excited state, we explored the possible correlation of σ_p^+, σ_p^- constants of the substituents in **5a–g** with the quantum yields and emission maxima of these analogues (Table 1).

The dependencies of quantum yields or emission wavelengths on Hammet substituent constants (σ_p, σ_p^+, σ_p^-) are given in Figure 5. An excellent correlation was found between the quantum yield values and σ_p^- constants ($R^2 = 0.94$) (Figure 5C), similar to that of σ_p (Figure 5A) and much better than correlation with σ_p^+ constants (Figure 5B). The data point for the $-NO_2$ substituted analogue **5e**, significantly deviates from all correlation graphs. The correlation of Φ values with σ_p^- constants implies that the electronic density redistribution in the excited states of the molecules generates partial negative charge.

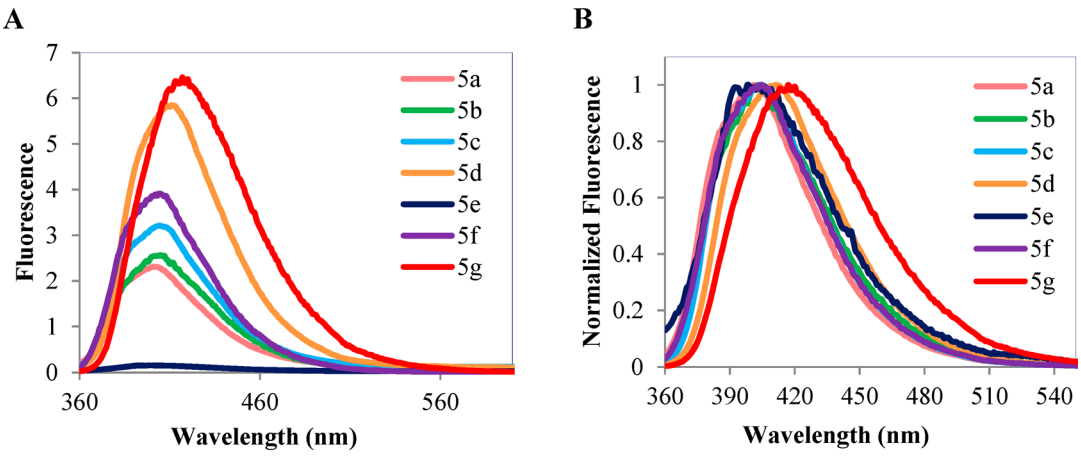

Figure 4. Fluorescence spectra (A) and normalized fluorescence spectra (B) for the series of *para*-substituted ^{Ph}ImC analogues in methanol (3 μM), λ_{ex} 350 nm.

dx.doi.org/10.1021/jo5011944 | J. Org. Chem. 2014, 79, 7051−7062

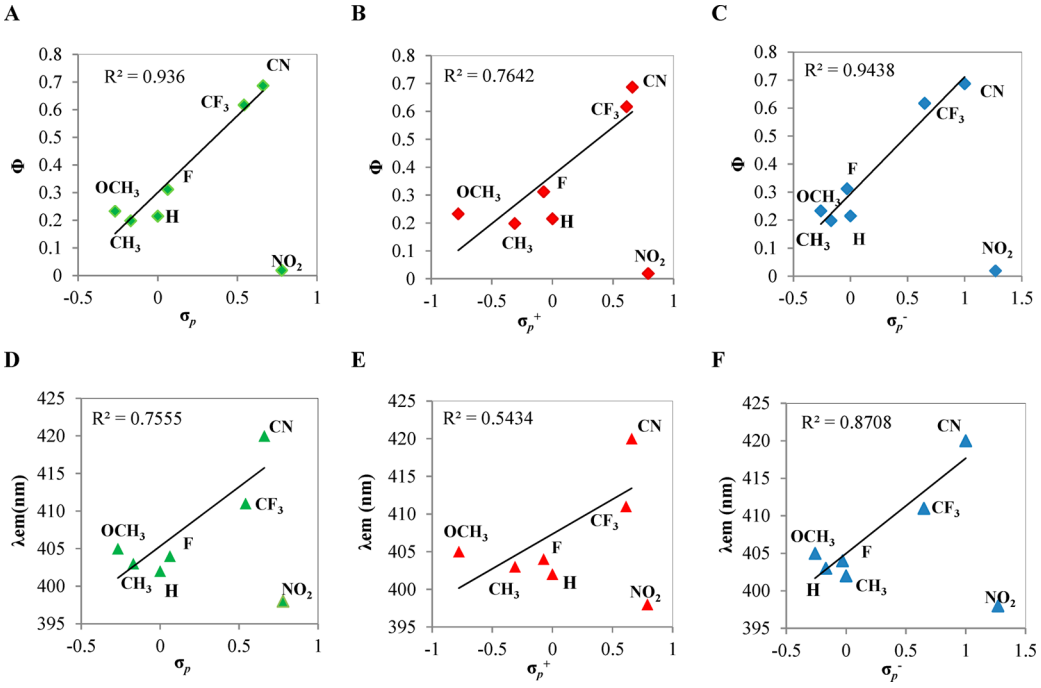

Figure 5. Correlation of quantum yields (**A**–**C**) or emission maxima (**D**–**F**) with σ constants (σ_p, σ_p^+, σ_p^-).

A plot of emission wavelengths vs σ_p^- (Figure 5F), indicated a linear dependence (R^2 = 0.87). Again the $-NO_2$-substituted analogue is an exception to this correlation. Previously, it was found that fluorescence decreases or even disappears upon introduction of a nitro group to fluorescent compounds.[18,59−61] The mechanism of quenching was related to the greatly lowered LUMO energy levels of the aromatic compounds due to the strong electron-withdrawing effect of nitro groups.[62] This finding is echoed in our results.

Effect of the Glycosyl Moiety on Photophysical Properties of 5d. In order to investigate the effect of the ribose ring on the fluorescence properties of phenyl-imidazolo-cytidine compounds, we synthesized imidazolo-cytosine and 2′-deoxy-cytidine analogues. Specifically, we synthesized analogues **6** and **7** because of the promising photophysical properties of CF_3-^{Ph}ImC, **5d**. Their quantum yields, absorption, and emission maxima are summarized in Table 2, and emission spectra are shown in Figure 6.

Table 2. Fluorescent Properties of ^{Ph}ImC Analogues 5d, 6, and 7

analogue	solvent	λ_{ab} (nm)	λ_{em} (nm)	Φ^a	ε ($cm^{-1}M^{-1}$)
5d	methanol	346	411	0.617	11250
6	water	332	416	0.712	9100
6	methanol	344	406	0.736	9350
7	methanol	347	405	0.642	10850

[a]Quantum yields were determined using quinine sulfate as a standard.

The ribose and 2′-deoxyribose rings reduced the quantum yield of the base analogue **6** in methanol by up to 17% (0.617 and 0.642 vs 0.736). However, only a minor change was observed in the emission wavelength due to the ribose/2′-deoxyribose ring (411 and 405 nm for **5d** and **7** vs 406 nm for **6**).

Due to the solubility of **6** in water fluorescence spectrum was also measured in an aqueous solution, showing small changes vs

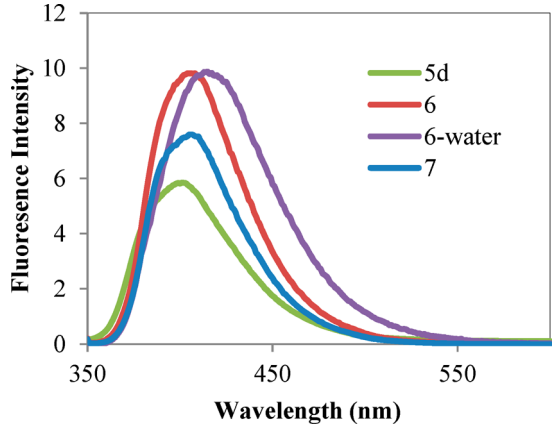

Figure 6. Fluorescence spectra for p-CF_3-substituted ^{Ph}ImC analogues (3 μM) in methanol (except for **6**, which was measured also in water at the same concentration).

that in methanolic solution. λ_{em} of **6** in water shifted to 416 nm vs 406 nm in methanol, and quantum yields were 0.712 in water vs 0.736 in methanol. We suggested that hydrogen bonding to **6** might play an important role in lowering the quantum yield. In methanol the less polar solvent, that less suited for hydrogen bonding with water, may explain the decrease of the quantum yield and the shift of λ_{em}. When we compared the fluorescence properties of **5d** to 2′-deoxycytosine analogue, **7**, as expected we observed very small change, due to the additional OH group.

The improved photophysical properties of **6** may suggest its potential use for the synthesis of fluorescent PNA (peptide nucleic acids) probes. In addition, the promising fluorescent properties of the 2′-deoxy-cytidine analogue **7** encouraged us to incorporate it into an oligonucleotide and to evaluate the potential of the latter as a probe for SNP detection (see below).

Theoretical Calculations. To better understand the effect of the substituents on the fluorescent properties of ^{Ph}ImC

dx.doi.org/10.1021/jo5011944 | J. Org. Chem. 2014, 79, 7051−7062

compounds, we explored the correlation between Φ of the latter compounds and their HOMO−LUMO energy gaps. Specifically, we studied model compounds *N*-Me-R-^{Ph}ImC **21a−e** and their four possible tautomers **A−D** (Figure 7). We

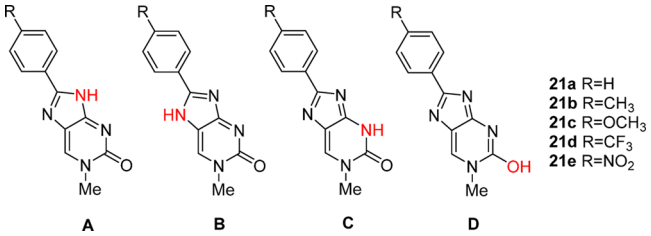

Figure 7. Four possible tautomers (**A−D**) of *N*-Me-R-^{Ph}ImC, **21a−e**.

calculated properties of models **21a−e** containing *N*-methyl group instead of a ribose group since the ribose group does not significantly affect the fluorescent properties of the modified base (Table 2).

The calculations focused on five substituents of ^{Ph}ImC that represent different electronic effects: strong electron withdrawing groups (-NO_2 and −CF_3), electron-donating groups (−OMe and −Me), and the parent compound.

Since ^{Ph}ImC has four possible tautomers, we first calculated their relative stabilities to determine their respective populations. We optimized each tautomer in the gas phase. For all substituents, tautomer **C** was the most stable. Tautomer **A** has higher energy than tautomer **C** (up to 2.6 kcal/mol for the −NO_2 substituent, **21e**). Tautomers **B** and **D** are destabilized by about 10 kcal/mol as compared to tautomer **C** (Table 3). This could possibly be due to repulsion between 1,3-nitrogen lone-pair electrons. Optimization of the tautomers in a continuum methanol solvent revealed that tautomer **A** is expected to be the dominant tautomer in methanol, while tautomer **C** is less stable than **A** by up to 1.8 kcal/mol (except for **21e**, where a mixture of tautomers **A** and **C** is expected). Tautomers **B** and **D** are the least stable forms also in methanolic solution (Table 3).

In addition, we computed the dipole moments for each tautomer both in gas and solution phases in an attempt to understand the above-mentioned effect of the solvent on tautomeric equilibrium. In all cases, tautomer B had the largest dipole moment, ca. 9−10 D, resulting in considerable stabilization of this tautomer in a polar solvent (methanol). This in turn induces a solvent effect on the tautomeric equilibrium (Table S41, Supporting Information). Indeed, the solvent induced change in the relative tautomerism energy is ca. 9 kcal/mol for all **B** analogues, resulting in similar energies for tautomers **A**, **B**, and **C**. Nonetheless, tautomers **A** and **C** remain more stable even in solution, and are expected to be the dominant forms.

Next, we explored the correlation between Φ and HOMO−LUMO energy gap of model compounds **21a−e**.[63] HOMO and LUMO orbital energies were calculated for the ground state in methanol. All calculations were performed on the most stable tautomer in methanol (tautomer **A** for −H, −CF_3, −CH_3 and tautomer **C** for −NO_2).

Table 4 presents experimental and computed absorption wavelengths and energies of HOMO and LUMO orbitals for compounds **21a−e**. In general, absorbance is related to the gap between HOMO and LUMO levels, and indeed the electronic transitions obtained from time-dependent (TD) DFT calculations are mainly composed of HOMO → LUMO transition (Table S41, Supporting Information). Yet, additional excitations also contribute to the first excited state. The oscillator strengths suggest that these are allowed transitions.

Derivatives **5d** and **5e** (−CF_3 and −NO_2 substituents, respectively) exhibited extremely high and low Φ values, respectively (Table 1). In an attempt to understand the effect of the substituents on the fluorescence of the nucleobases, one may analyze the frontier orbital energy levels and their spatial distribution. In a previous study on a series of 8-(substituted cinnamyl)-adenosine derivatives, we have shown that the electron density of LUMO orbitals of nitro-compounds is largely localized on the benzene ring, due to the strong electron withdrawing effect of the substituent.[18] Here, we observed the same pattern of large localization of electron density on the benzene ring in LUMO of derivative **21e** due to the nitro group (Figure 8).[62]

The small energy gap of the HOMO−LUMO levels (Table 4) of the nitro derivative leads to a possible quenching channel of the fluorescence. Thus, we suggest that the HOMO−LUMO gap in model compound **21e**, which is smaller than for all other model compounds, explains its Φ value which was found to be an order of magnitude lower than that of all other compounds.

Incorporation of ^{Ph}ImC Analogue 7 into an Oligonucleotide. To explore potential applications of ^{Ph}ImC compounds, we studied the photophysical properties of derivative **5d** within a DNA environment. We selected *p*-CF_3-substituted analogue, **5d**, which showed one of the highest quantum yields and relatively long absorption and emission wavelengths (λ_{ex} 346 nm, λ_{em} 411 nm, Φ 0.617). Previously, we showed by NMR studies, that analogue **5d** preserves cytidine natural hydrogen bond pattern with guanosine.[27] Here we extended our studies and explored the tautomeric equilibrium of **5d** in methanol solution by calculations at M062X/6-311++G(d,p) level (Table 3). Tautomer **A**, which resembles cytidine in Watson−Crick base-pairing with guanosine, was found to be the most stable among the possible tautomers (Figure 7). However, tautomer **C**, which resembles uridine in Watson−

Table 3. Relative Energies (kcal/mol) in the Gas Phase and in Methanol Solution for 21a−e Obtained from Calculations Performed at M062X/6-311++G(d,p) level

		gas phase				methanolic solution			
	R	A	B	C	D	A	B	C	D
21a	H	0.47	9.54	0.00	10.46	0.00	2.71	1.45	9.55
21b	CH_3	0.72	9.22	0.00	10.55	0.00	2.65	1.81	9.95
21c	OCH_3	1.38	9.70	0.00	10.58	0.00	1.28	1.28	9.29
21d	CF_3	2.09	11.18	0.00	10.06	0.00	3.53	0.95	8.95
21e	NO_2	2.59	12.11	0.00	9.85	0.00	3.11	0.18	7.75

dx.doi.org/10.1021/jo5011944 | J. Org. Chem. 2014, 79, 7051−7062

Table 4. Absorption Wavelengths (λ_{abs}), Oscillator Strengths (f), Molecular Orbital Energies, and Molecular Orbital Energy Gaps, Obtained from Calculations Performed at the M062X/6-311++G(d,p) Level in Methanol Solution

analogue	R	λ_{abs} (nm) expt	λ_{abs} (nm) calcd	f	HOMO (eV)	LUMO (eV)	Δ (eV)	Φ expt
21a	H	342	314	0.526	−0.2715	−0.0498	0.220	0.215
21b	CH_3	344	314	0.571	−0.2695	−0.0472	0.222	0.198
21c	OCH_3	347	317	0.620	−0.2648	−0.0450	0.220	0.233
21d	CF_3	346	317	0.567	−0.2763	−0.0579	0.218	0.617
21e	NO_2	368	345	0.764	−0.2777	−0.0855	0.190	0.019

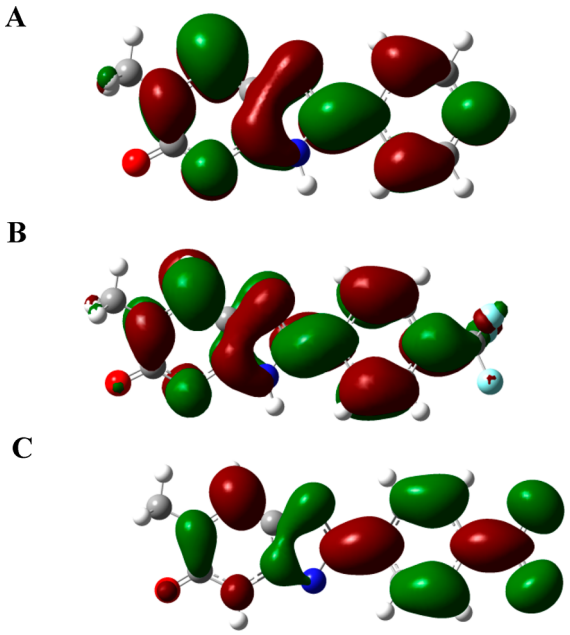

Figure 8. LUMO orbitals of compounds **21a**, **21d**, and **21e**: (A) **21a** (−H) (B) **21d** (−CF_3), (C) **21e** (−NO_2).

Crick base-pairing with adenosine, was also quite stable with relative energy of 0.95 kcal/mol. To obtain experimental support for the compatibility of **5d** to cytidine in DNA, we prepared phosphoramidite monomer **20** for incorporation into DNA probe.

Prior to the spectroscopic studies of DNA modified with CF_3-^{Ph}ImdC, **7**, we wanted to investigate the potential quenching of **5d** in the presence of various nucleobases. For this purpose we performed Stern−Volmer titration of **5d** with all 5′-monophosphate nucleotides (NMPs) (Figure S3, Supporting Information). We observed minor fluorescence quenching of **5d** with CMP and no quenching with UMP. AMP and particularly GMP induced significant fluorescence quenching. These results imply that **5d** may be a good candidate for mismatch detection.

Next, we incorporated CF_3-^{Ph}ImdC, **7**, into a 15-mer oligonucleotide (Figure 9). Solid-phase oligonucleotide synthesis was performed by employing phosphoramidite **20** and standard building blocks. We incorporated this monomer at the center of oligodeoxynucleotide (ODN) in order to study its photophysical properties both in a single stranded DNA and in the corresponding duplexes with either DNA or RNA (oligoribonucleotide (ORN)). Furthermore, we investigated the influence of **7** on the stability of both complementary and noncomplementary (mismatched) duplexes. For this purpose, we used the oligonucleotides shown in Figure 9.

The absorption and fluorescence spectra of **ODN(CF$_3$-^{Ph}ImdC)** probe and the corresponding duplexes were measured at 25 °C at 2 μM concentration in PBS buffer at pH 7.4. **ODN(CF$_3$-^{Ph}ImdC)** exhibited an absorption band at 343 nm similar to **7**, and upon duplex formation the absorption maxima shifted slightly to a longer wavelength (350 nm) (Figure 10).

The emission spectrum of **ODN(CF$_3$-^{Ph}ImdC)** shows a signal at 406 nm, however, its quantum yield decreased 6-fold as compared to that of 2′-deoxy nucleoside **7** (0.102 vs 0.642) (Table 5). In the duplexes of **ODN(CF$_3$-^{Ph}ImdC)**, with matched and mismatched strands, the fluorescence of **7** was strongly dependent on the purine base paired to it. Thus, the quantum yield of mismatched **ODN(CF$_3$-^{Ph}ImdC):ODN(A)** was reduced 2-fold vs that of **ODN(CF$_3$-^{Ph}ImdC)**, while mismatched **ODN(CF$_3$-^{Ph}ImdC):ODN(C)/(T)** resulted in 6.5-fold reduction of fluorescence. The most impressive effect was observed for matched **ODN(CF$_3$-^{Ph}ImdC):ODN(G)**, where the fluorescence of the duplex was reduced 16.5-fold vs that of the single strand, **ODN(CF$_3$-^{Ph}ImdC)**. Interestingly, the corresponding duplex with RNA, **ODN(CF$_3$-^{Ph}ImdC):ORN(G)**, showed a 11.5-fold higher quantum yield vs its DNA counterpart (0.027 vs 0.006). These observations suggest that **ODN(CF$_3$-^{Ph}ImdC)** may be used as a sensitive, DNA-selective, SNP probe.

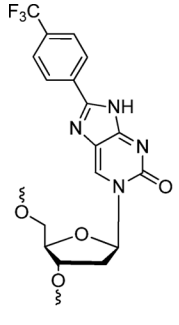

CF_3-^{Ph}ImdC

ODN(C)	5'- AGTGGACCTGAAGAA-3'	**unmodified**
ODN(CF$_3$-^{Ph}ImdC)	5'- AGTGGAC**CF$_3$-^{Ph}ImdC** TGAAGAA-3'	
ODN(G)	3'- TCACCTG**G**TGTTCTT -5'	**match**
ODN(A)	3'- TCACCTG**A**TGTTCTT -5'	**mismatch-A**
ODN(C)	3'- TCACCTG**C**TGTTCTT -5'	**mismatch-C**
ODN(T)	3'- TCACCTG**T**TGTTCTT -5'	**mismatch-T**
ORN(G)	3'- UCACCUG**G**UGUUCUU-5'	**match**

Figure 9. Sequences of matched and mismatched ODNs used for study of **ODN(CF$_3$-^{Ph}ImdC)**.

dx.doi.org/10.1021/jo5011944 | J. Org. Chem. 2014, 79, 7051−7062

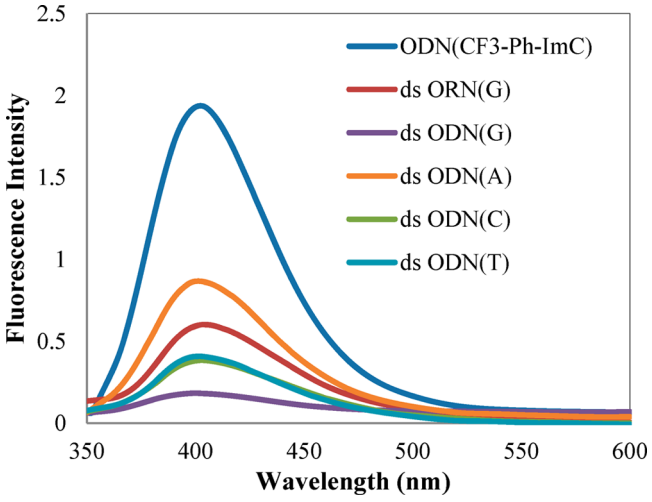

Figure 10. Fluorescence spectra for CF_3-^{Ph}ImdC-labeled **ODN** and the corresponding duplexes. All measurements were carried out at 2 μM in PBS buffer (pH 7.4) at room temperature, λ_{ex} 350.

Table 5. Photophysical Properties of ODN(CF_3-^{Ph}ImdC) and the Corresponding Duplexes[a]

	λ_{abs} (nm)	λ_{em} (nm)	Φ	T_m (°C)
single strand **ODN(CF_3-^{Ph}ImdC)**	343	406	0.102	
duplex with **ODN(G)**	350	405	0.006	43
duplex with **ODN(A)**	348	403	0.049	39
duplex with **ODN(C)**	347	402	0.014	39
duplex with **ODN(T)**	348	403	0.016	41
duplex with **ORN(G)**	348	401	0.027	46
unmodified DNA duplex				44

[a]All measurements were carried out at 2 μM in PBS buffer (pH 7.4) at room temperature.

The T_m values of the matched and mismatched duplexes compared with the unmodified duplex, are presented in Table 5. Apparently, CF_3-^{Ph}ImdC can form stable base pairing interactions in both DNA and RNA duplexes. The T_m values of matched **ODN(CF_3-^{Ph}ImdC):ODN(G)/ORN(G)** duplexes were similar to unmodified duplex (43 and 46 vs 44 °C), while T_m of mismatched duplexes was lower than that of unmodified duplex (39 and 41 °C vs 44 °C).

The above calculations indicated that more stable tautomer of **CF_3-^{Ph}ImdC** fluorescent analogue is **A**, similar to cytidine structure. We assumed that tautomer **A** is also stable in duplex environment. This assumption was confirmed by the fact that the matched duplex **ODN(CF_3-^{Ph}ImdC):ODN(G)** had T_m, almost identical to unmodified duplex. The mismatched duplex with **ODN(A)** had lower T_m than the matched duplex possibly indicating that the base-paired tautomer **C**, that is more similar to uridine structure, is less stable in duplex environment. In addition, we observed a larger decrease of quantum yield in **ODN(CF_3-^{Ph}ImdC):ODN(G)** matched duplex vs mismatched duplexes indicating stronger hydrogen bonding. Since hydrogen bonding has significant effect on quantum yield, we concluded that the more stable tautomer of CF_3-^{Ph}ImdC in duplex environment is **A**.

Only a few methods of mismatched detection based on fluorescence of the opposing nucleotide have been reported in the literature, and even fewer exhibited a significant change in quantum yield and emission wavelengths.[64−67] Our data indicate that **ODN(CF_3-^{Ph}ImdC)** is appropriate for discrimination between natural base-pairing and mismatched pairing. Furthermore, ODN (CF_3-^{Ph}ImdC) was found to be highly selective for DNA vs RNA.

CONCLUSIONS

We reported here on the synthesis of a series of fluorescent ^{Ph}**ImC** analogues. Next, we established a correlation between the nature of *para*-substituents of the phenyl ring and the fluorescent properties of these analogues, **5a−g**. A linear dependence was observed between Φ or emission wavelength values and σ_p^- values (R^2 = 0.94 and 0.87, respectively).

DFT calculations of model compounds **21a−e** helped identify the most stable tautomers in methanol solution, and provided rational for the low fluorescence of the nitro derivative. The calculations suggest two dominant tautomers (**A** and **C**) in methanol solution. Moreover, the computed absorption lines are in fair agreement with experiment, and the low fluorescence of the nitro compound is possibly due to the narrow HOMO−LUMO energy gap, which could open a nonradiative decay channel.

p-CF_3-^{Ph}ImdC, **7**, which proved to be one of the most promising fluorescent probes in ImC series, was incorporated into an oligonucleotide. This fluorescent cytidine analogue exhibited 8025-fold higher quantum yield (Φ 0.642) as compared to cytidine. Analogue **7** did not interfere with the hybridization process (ΔT_m = 1 °C between **ODN(CF_3-^{Ph}ImdC):ODN(G)**, and the native duplex), thus supporting the predominance of tautomer **A** of analogue **7**. Moreover, A *17-fold* reduction of fluorescence was observed for the *G-matched* duplex vs **ODN(CF_3-^{Ph}ImdC)**, while for *A-mismatched* duplex, only a *2-fold* decrease was observed. Usually, the most common mutation is the transition that exchanges a purine for a purine, A to G or vice versa. Hence, our data suggest that **ODN(CF_3-^{Ph}ImdC)** probe can be used to detect DNA single mismatch. Furthermore, since quantum yield of **ODN(CF_3-^{Ph}ImdC):ODN(G)** was reduced 17-fold vs that of single strand, whereas quantum yield of the corresponding **ODN(CF_3-^{Ph}ImdC):ORN(G)** was reduced only 3.8-fold, **ODN(CF_3-^{Ph}ImdC)** appears to be a DNA-selective probe.

To conclude, CF_3-^{Ph}ImdC-labeled probes have a potential for SNP typing; however, more studies are required to establish their potential. In particular, the required studies include incorporation of additional phenyl-imidazolo-cytidine analogues into different positions in a DNA sequence and analysis of their photophysical properties. These studies will be reported in due course.

EXPERIMENTAL SECTION

General Methods. Reagents and solvents were purchased from commercial sources and were used without further purification. All moisture-sensitive reactions were carried out in flame-dried reaction flasks with rubber septa, and the reagents were introduced with a syringe. All reactants in moisture-sensitive reactions were dried overnight in a vacuum oven. Progress of the reactions was monitored by TLC on precoated silica gel plates. Visualization was accomplished by UV light. Flash chromatography was carried out on silica gel. Medium pressure chromatography was carried out using automated flash purification system. ^{1}H NMR spectra were obtained using a 200, 300, 400, or 600 MHz spectrometer. ^{13}C NMR spectra were obtained at 75, 100, or 150 MHz spectrometer. Chemical shifts are expressed in ppm downfield from Me_4Si (TMS) used as internal standard. The values are given in δ scale. New compounds were analyzed under ESI

dx.doi.org/10.1021/jo5011944 | J. Org. Chem. 2014, 79, 7051−7062

(electron spray ionization) conditions on a Q-TOF microinstrument. High resolution MS-MALDI-TOF spectra were recorded with TOF/TOF instrument. Absorption spectra were measured on a UV instrument using a 1 cm path length quartz cell. Emission spectra were measured using luminescence spectrometer, and the emission was corrected for the monochromator sensitivity according to the standard procedure. Oligonucleotides were synthesized by standard automated solid-phase method.

General Procedure for Synthesis of Protected *Para*-Substituted Phenyl-imidazolo-cytidine Derivatives 10e−g. Protected 5-NH_2-cytidine, **8** (100 mg, 0.17 mmol), and the appropriate *para*-substituted benzaldehyde (0.20 mmol) were thoroughly mixed in DMF (2 mL), then *p*-TsOH (7 mg, 0.034 mmol) was added, and the solution was heated and stirred at 80 °C for 2−4 h and monitored by TLC ($CHCl_3$/MeOH 9.5:0.5). When the reaction was completed, the solution was cooled to rt. The reaction mixture was added dropwise with vigorous stirring into a mixture of Na_2CO_3 (0.034 mmol) and H_2O (10 mL). The crude product was extracted into EtOAc. The organic phase was washed with H_2O and brine and dried (Na_2SO_4). Evaporation of solvent gave the crude product, which was purified by column chromatography over silica gel (9:1 DCM/EtOH).

***p*-Nitrophenyl-imidazolo-cytidine-2′,3′,5′-*O*-tribenzoate (10e).** Product **10e** was obtained by condensation of **8** (100 mg, 0.17 mmol) with *p*-nitrobenzaldehyde **9e** (31 mg, 0.20 mmol) with *p*-TsOH (7 mg, 0.034 mmol) as a catalyst, according to the general procedure. Product **10e** was obtained as a white solid in 40% yield (48 mg). Mp: 172−174 °C. ^{1}H NMR (600 MHz, $CDCl_3$): δ 8.74 (s, 1H), 8.63 (d, 2H), 8.30 (d, *J*=8.4 Hz, 2H), 8.12 (d, *J*=7.7 Hz, 2H), 8.07 (d, *J*=7.7 Hz, 2H), 7.94 (d, *J*=7.7 Hz, 2H), 7.55 (m, 3H), 7.42 (m, 4H), 7.36 (m, 2H), 6.47 (bs, 1H), 6.15 (m, 1H), 5.90 (m, 1H), 4.88 (m, 3H) ppm. ^{13}C NMR (150 MHz, $CDCl_3$): δ 166.1, 165.2, 165.0, 162.7, 154.4, 149.4, 135.5, 133.8, 133.4, 129.9, 129.8, 129.5, 129.2, 128.9, 128.7, 128.6, 128.5, 128.4, 128.2, 126.2, 124.2, 91.9, 80.5, 75.0, 70.1, 63.1 ppm. HRMS (MALDI-TOF) *m*/*z*: calcd for $C_{37}H_{27}N_5O_{10}Na$ 724.1655 [M + Na^+], found 724.1648 [M + Na^+].

***p*-Fluorophenyl-imidazolo-cytidine-2′,3′,5′-*O*-tribenzoate (10f).** Product **10f** was obtained by condensation of **8** (100 mg, 0.17 mmol) with *p*-fluorobenzaldehyde **9f** (25 mg, 0.20 mmol) with *p*-TsOH (7 mg, 0.034 mmol) as a catalyst, according to general procedure. Product **10f** was obtained as a white solid in 45% yield (51 mg). Mp: 183−185 °C. ^{1}H NMR (300 MHz, $CDCl_3$): δ 8.75 (s, 1H), 8.52 (m, 2H), 8.24 (d, *J*=7.8 Hz, 2H), 8.13 (m, 2H), 8.07 (m, 4H), 7.68 (m, 2H), 7.56 (m, 7H), 7.26 (m, 2H), 6.55 (m, 1H), 6.21 (m, 1H), 6.04 (m, 1H), 5.03 (m, 3H) ppm. ^{13}C NMR (75 MHz, $CDCl_3$): δ 166.1, 165.2, 165.0, 163.3, 162.6, 134.1, 133.7, 133.6, 133.3, 130.4, 129.8, 129.1, 128.6, 128.5, 128.4, 123.9, 116.4, 116.1, 115.8, 92.3, 80.4, 75.1, 70.4, 63.4 ppm. HRMS (MALDI-TOF) *m*/*z*: calcd for $C_{37}H_{28}FN_4O_8$ 675.1889 [M + H^+], found 675.1886 [M + H^+].

***p*-Cyanophenyl-imidazolo-cytidine-2′,3′,5′-*O*-tribenzoate (10g).** Product **10g** was obtained by condensation of **8** (100 mg, 0.17 mmol) with *p*-cyanobenzaldehyde **9g** (27 mg, 0.20 mmol) with *p*-TsOH (7 mg, 0.034 mmol) as a catalyst, according to the general procedure. Product **10g** was obtained as a white solid in 41% yield (56 mg). Mp: 183−185 °C. ^{1}H NMR (400 MHz, $CDCl_3$): δ 8.83 (s, 1H), 8.60 (m, 2H), 8.25 (d, *J*=7.4 Hz, 2H), 8.10 (m, 4H), 7.82 (d, *J*=7.7 Hz, 2H), 7.80 (m, 3H), 7.71 (m, 6H), 6.54 (m, 1H), 6.24 (m, 1H), 6.04 (m, 1H), 5.06 (m, 3H) ppm. ^{13}C NMR (100 MHz, $CDCl_3$): δ 166.1, 165.2, 165.0, 162.4, 155.6, 154.5, 135.5, 133.9, 133.7, 133.4, 132.7, 129.9, 129.8, 129.7, 129.1, 128.9, 128.8, 128.6, 128.5, 128.4, 128.3, 126.2, 118.3, 114.7, 92.1, 80.6, 75.1, 70.3, 63.2 ppm. HRMS (MALDI-TOF) *m*/*z*: calcd for $C_{38}H_{28}N_5O_8$ 682.1938 [M + H^+], found 682.1932 [M + H^+].

General Procedure for Synthesis of Imidazolo-cytidine Derivatives 5e−g. Protected nucleoside (0.15 mmol, 1 equiv) was added to a solution of NaOH (54 mg, 1.35 mmol, 9 equiv) in MeOH (2 mL), and the resulting mixture was stirred at room temperature for 1 h. The residue was diluted with dichloromethane and extracted with water, and the aqueous layer was freeze-dried. The crude product was purified by an automated medium pressure column chromatography (8:2 $CHCl_3$/MeOH).

***p*-Nitrophenyl-imidazolo-cytidine (5e).** Product **5e** was obtained by treating protected nucleoside **10e** (105 mg, 0.15 mmol) with NaOH in MeOH according to general procedure, yielding 52 mg (85%) of a white solid. Mp: >222 °C dec. ^{1}H NMR (600 MHz, DMSO-d_6): δ 8.99 (s, 1H), 8.36 (d, *J* = 7.2 Hz, 2H), 8.24 (d, *J* = 7.2, 2H), 5.89 (d, *J* = 2.2 Hz, 1H), 5.55 (s, 1H), 5.41 (s, 1H), 5.03 (s, 1H), 4.05 (m, 2H), 3.97 (m, 1H), 3.84 (m, 1H), 3.67 (m, 1H) ppm. ^{13}C NMR (150 MHz, DMSO-d_6): δ 155.4, 154.8, 148.8, 138.5, 135.6, 131.8, 126.2, 123.8, 92.2, 85.1, 75.1, 68.8, 59.9 ppm. HRMS (MALDI-TOF) *m*/*z*: calcd for $C_{16}H_{15}N_5O_7Na$ 412.0869 [M + Na^+], found 412.0871 [M + Na^+].

***p*-Fluorophenyl-imidazolo-cytidine (5f).** Product **5f** was obtained by treating protected nucleoside **10f** (100 mg, 0.15 mmol) with NaOH in MeOH according to general procedure, yielding 47 mg (87%) of a yellowish solid. Mp: >212 °C dec. ^{1}H NMR (400 MHz, DMSO-d_6): δ 9.08 (s, 1H), 8.19 (m, 2H), 7.38 (m, 2H), 5.91 (d, *J* = 2.7 Hz, 1H), 5.54 (s, 1H), 5.38 (s, 1H), 5.06 (s, 1H), 4.06 (m, 2H), 3.97 (m, 1H), 3.84 (m, 1H), 3.68 (m, 1H) ppm. ^{13}C NMR (100 MHz, DMSO-d_6): δ 164.8, 162.4, 162.2, 153.7, 134.3, 131.7, 131.6, 129.3, 129.2, 128.1, 126.0, 124.9, 116.2, 115.9, 114.8, 114.6, 91.2, 83.9, 75.1, 70.3, 69.1, 59.4 ppm. HRMS (MALDI-TOF) *m*/*z*: calcd for $C_{16}H_{15}FN_4O_5Na$ 385.0924 [M + Na^+], found 385.0923 [M + Na^+].

***p*-Cyanophenyl-imidazolo-cytidine (5g).** Product **5g** was obtained by treating protected nucleoside **10g** (102 mg, 0.15 mmol) with NaOH in MeOH according to general procedure, yielding 46 mg (80%) of a white solid. Mp: >205 °C dec. ^{1}H NMR (400 MHz, DMSO-d_6): δ 8.89 (s, 1H), 8.41 (d, *J* = 8.1 Hz, 2H), 7.91 (d, *J* = 8.1, 2H), 5.90 (d, *J* = 2.3 Hz, 1H), 5.61 (s, 1H), 5.42 (s, 1H), 5.04 (s, 1H), 4.04 (m, 2H), 3.99 (m, 1H), 3.90 (m, 1H), 3.73 (m, 1H) ppm. ^{13}C NMR (100 MHz, DMSO-d_6): δ 163.4, 137.5, 131.6, 128.7, 128.6, 124.3, 123.4, 91.2, 83.7, 74.1, 67.5, 58.9 ppm. HRMS (MALDI-TOF) *m*/*z*: calcd for $C_{17}H_{15}N_5O_5Na$ 392.0971 [M + Na^+], found 392.0990 [M + Na^+].

5-Amino-cytosine (13). 5-Nitro-cytosine **12** (2 g, 12.8 mmol) and 10% Pd−C (140 mg) in H_2O/EtOH (2:1, 20 mL) was shaken in Parr apparatus under H_2 atmosphere (55 psi) for 3 h. The suspension was filtered over Celite and washed with hot water. The filtrate was concentrated in vacuo. The crude product was recrystallized from water. The green crystals was filtered and washed with ice-cold water to give 1.2 g (75%) of product **13**. Mp: 247−249 °C. ^{1}H NMR (300 MHz, DMSO-d_6): δ 10.01 (br. s, 2H), 6.74 (s, 1H), 6.62 (br. s, 1H), 3.80 (s, 2H) ppm. ^{13}C NMR (150 MHz, DMSO-d_6): δ 162.2, 156.1, 124.3, 115.3 ppm. HRMS (MALDI-TOF) *m*/*z*: calcd for $C_4H_7N_4O_1$ 127.0620 [M + H^+], found 127.0629 [M + H^+].

***p*-(Trifluoromethyl)phenyl-imidazolo-cytosine (6).** 5-Amino-cytosine, **13** (300 mg, 2.36 mmol), and *p*-trifluoromethylbenzaldehyde (330 mg, 3.00 mmol) were thoroughly mixed in DMF (15 mL), *p*-TsOH (81 mg, 0.47 mmol) was added, and the solution was heated and stirred at 80 °C for 6 h and monitored by TLC ($CHCl_3$/MeOH, 8:2). When the reaction was completed, the solution was cooled to rt. Evaporation of the solvent gave the crude product, which was purified by column chromatography over silica gel, yielding 364 mg (55%) of a white solid. Mp: >218 °C dec. ^{1}H NMR (600 MHz, DMSO-d_6): δ 8.46 (s, 1H), 8.33 (d, *J* = 6.4 Hz, 2H), 7.89 (d, *J* = 6.4, 2H) ppm. ^{13}C NMR (150 MHz, DMSO-d_6): δ 132.3, 131.2, 128.9, 128.3, 127.1, 127.0, 126.1 ppm. HRMS (MALDI-TOF) *m*/*z*: calcd for $C_{12}H_8F_3N_4O$ 281.0650 [M + H^+], found 281.0639 [M + H^+].

5-Nitro-2′-deoxyuridine-3′,5′-O-diacetate (15). 2′-Deoxyuridine, **14** (5 g, 0.02 mol), was treated with acetic anhydride (11 μL, 0.12 mol) in pyridine (200 mL) at room temperature overnight. Volatiles were evaporated to dryness, and the residue was coevaporated from toluene to remove traces of pyridine, acetic acid, and acetic anhydride. Acetylated uridine was obtained as gammy solid without purification, yielding 5.2 g, 95%. The acetylated nucleoside was dissolved in dimethylformamide (150 mL) and treated with nitrosonium tetrafluoroborate (14 g, 0.11 mol) for 30 min. The reaction was terminated by addition of water (20 mL). The reaction mixture was diluted with ethyl acetate (600 mL) and washed with

dx.doi.org/10.1021/jo5011944 | J. Org. Chem. 2014, 79, 7051−7062

aqueous sodium bicarbonate. The organic layer was separated and dried over sodium sulfate. The crude product was purified on a silica gel column using ethyl acetate/hexanes (1:1 v/v). Fractions containing the titled product were combined and evaporated to give 7.2 g (92%). Mp: 175−177 °C. ^{1}H NMR (600 MHz, $CDCl_3$): δ 9.11 (s, 1H), 8.78 (s, 1H), 6.28 (m, 1H), 5.26 (m, 1H), 4.40 (m, 3H), 2.71 (m, 1H) 2.30 (m, 1H), 2.16 (s, 3H), 2.13 (s, 3H) ppm. ^{13}C NMR (150 MHz, $CDCl_3$): δ 170.3, 170.2, 153.4, 147.8, 143.7, 126.1, 86.8, 83.5, 73.7, 63.5, 39.1, 20.8, 20.7 ppm. HRMS (MALDI-TOF) m/z: calcd for $C_{13}H_{15}N_3O_9Na$ 380.0703 [M + Na^+], found 380.0706 [M + Na^+].

5-Nitro-2′-deoxycytidine-3′,5′-*O*-diacetate (16). 5-Nitro-uridine-3′,5′-O-diacetate, **15** (1 g, 2.82 mmol), was dissolved in dry acetonitryle (50 mL). Triethylamine (1 mL, 7.17 mmol) and 2-mesitylenesulfonyl chloride (1.1 g, 5.41 mmol) were added, and the mixture was left at room temperature for 3 h. Next, a mixture of 1:1 NH_4OH/CH_3CN (17 mL) was added and the reaction was stirred for additional 3 h at room temperature. The reaction mixture was diluted with dichloromethane and washed with 1 M $KHSO_4$ solution. The organic layer was separated, washed twice with water, dried over sodium sulfate, and evaporated. The crude product was purified on a silica gel column using ethyl acetate/methanol (9:1 v/v). Fractions containing the titled product were combined and evaporated to give a pure nucleoside as yellowish foam (678 mg, 68%). Mp: 178−179 °C. ^{1}H NMR ($CDCl_3$): δ 9.22 (s, 1H), 7.92 (s, 1H), 8.03 (s, 1H), 6.88 (s, 1H), 6.23 (m, 1H), 5.22 (m, 1H), 4.41 (m, 3H), 2.85 (m, 1H), 2.22 (m, 1H), 2.14 (s, 3H), 2.11 (s, 3H) ppm. ^{13}C NMR (150 MHz, $CDCl_3$): δ 170.3, 170.2, 157.7, 152.1, 145.5, 119.6, 87.8, 83.3, 73.93, 63.3, 39.6, 20.8, 20.6 ppm. HRMS (MALDI-TOF) m/z: calcd for $C_{13}H_{16}N_4O_8Na$ 379.0866 [M + Na^+], found 379.0865 [M + Na^+].

5-Amino-2′-deoxycytidine-3′,5′-*O*-diacetate (17). To a solution of **16** (1 g, 2.8 mmol) in THF (104 mL), and glacial AcOH (8 mL) was added 10% Pd/C (625.5 mg). The solution was charged with H_2 (1.5 atm), and stirred for 7 h at room temperature. The reaction was filtered through a pad of Celite, washed with an excess of MeOH, and concentrated in vacuo. The crude material was purified by automated column chromatography (20% MeOH in EtOAc) yielding **17** (450 mg, 50%). Mp: 188−190 °C. ^{1}H NMR (600 MHz, $CDCl_3$): δ 7.26 (s, 1H), 7.12 (s, 1H), 6.26 (m, 1H), 5.14 (m, 1H), 4.28 (m, 2H), 4.17 (m, 1H), 2.47 (m, 1H), 2.12 (m, 1H), 2.05 (s, 6H) ppm. ^{13}C NMR (150 MHz, $CDCl_3$): δ 170.5, 170.4, 162.0, 154.6, 125.0, 115.6, 85.7, 81.7, 74.2, 63.8, 37.4, 20.8, 20.7 ppm. HRMS (MALDI-TOF) m/z: calcd for $C_{13}H_{18}N_4O_6Na$ 349.1124 [M + Na^+], found 349.1119 [M + Na^+].

***p*-(Trifluoromethyl)phenyl-imidazolo-2′-deoxycytidine-3′,5′-*O*-diacetate (18).** Protected 5-amino-2′-deoxycytidine **17** (540 mg, 1.65 mmol) and *p*-TsOH (70 mg, 0.33 mmol) were thoroughly mixed in DMF (5.5 mL), *p*-(trifluoromethyl)benzaldehyde (260 μL, 1.90 mmol) then was added, and the solution was heated and stirred at 80 °C for 2 h. The reaction mixture was cooled to rt and added dropwise with vigorous stirring into a mixture of K_2CO_3 (320 mg, 2.31 mmol) and H_2O (10 mL). The crude product was extracted into EtOAc, and the organic phase was washed with H_2O and brine and dried (Na_2SO_4). Evaporation of solvent gave the crude product, which was purified by column chromatography over silica gel (1% MeOH in EtOAc) yielding **18** (435 mg, 50%). Mp: 184−185 °C. ^{1}H NMR (600 MHz, $CDCl_3$): δ 8.71 (s, 1H), 8.55 (d, J = 6.4 Hz 2H), 7.78 (d, J = 6.4 Hz, 2H), 6.27 (m, 1H), 5.27 (m, 1H), 4.43 (m, 2H), 4.29 (m, 1H), 2.78 (m, 1H), 2.16 (m, 1H), 2.11 (s, 6H) ppm. ^{13}C NMR (150 MHz, $CDCl_3$): δ 170.4, 170.2, 162.6, 161.5, 156.1, 154.6, 135.0, 134.6, 133.4, 133.1, 132.9, 132.7, 131.1, 129.9, 128.2, 128.1, 126.0, 125.4, 124.6, 122.8, 121.0, 88.6, 83.3, 73.7, 63.5, 39.2, 20.8, 20.7 ppm. HRMS (MALDI-TOF) m/z: calcd for $C_{21}H_{20}F_3N_4O_6$ 481.1335 [M + H^+], found 481.1344 [M + H^+].

***p*-(Trifluoromethyl)phenyl-imidazolo-2′-deoxycytidine (7).** Compound **18** (300 mg, 0.63 mmol) was dissolved in NaOH (75 mg, 1.87 mmol) solution in methanol (8 mL) and stirred at room temperature for 3 h. The reaction was neutralized with acetic acid and evaporated. The crude product was purified by column chromatography over silica gel (DCM/EtOH, 4:3) yielding 7 (185 mg, 80%). Mp: >205 °C dec. ^{1} H NMR (400 MHz, DMSO-d_6): δ 9.02 (s, 1H), 8.38 (d, J = 7.27 Hz, 2H), 7.92 (d, J = 7.27 Hz, 2H), 6.25 (m, 1H), 5.27 (m, 1H), 4.28 (m, 1H), 3.74 (m, 1H), 3.67 (m, 1H), 3.64 (m, 2H), 2.42 (m, 1H), 2.15 (m, 1H). ^{13}C NMR (100 MHz, DMSO-d_6): δ 153.6, 135.1, 127.4, 125.8, 125.2, 87.9, 87.2, 69.4, 60.5, 41.4 ppm. HRMS (MALDI-TOF) m/z: $C_{17}H_{16}F_3N_4O_4$ 397.1123 [M + H^+], found 397.1128 [M + H^+].

***p*-(Trifluoromethyl)phenyl-imidazolo-(2′-deoxy-5′-O-dimethoxytrityl)-cytidine (19).** Compound 7 (100 mg, 0.25 mmol) was coevaporated twice with dry pyridine and then dissolved in the same solvent (1 mL). 4,4′-Dimethoxytrityl chloride (102 mg, 1.51 mmol) was dissolved in dry pyridine (1 mL) and added dropwise to the solution which was stirred at room temperature for 2 h. Methanol (0.5 mL) was added, and the solution was evaporated. The residue was coevaporated twice with toluene and then purified by column chromatography over silica gel (DCM/MeOH, 95:5 containing 1% pyridine) yielding **19** (110 mg, 65%). Mp: 215−217 °C. ^{1}H NMR (600 MHz, Acetone-d_6): δ 8.78 (s, 1H). 8.48 (d, J = 8.7 Hz, 2H), 7.87 (d, J = 8.7 Hz, 2H), 7.54 (m, 2H), 7.46 (m, 2H), 7.42 (m, 2H), 7.32 (t, J = 6.5, 2H), 7.21 (t, J = 6.1, 1H), 6.91 (m, 4H), 6.34 (t, J = 5.9 1H), 4.62 (m, 1H), 4.25 (m, 1H), 3.76 (s, 3H), 3.73 (s, 3H), 3.53 (m, 1H), 3.44 (m, 1H), 2.73(m, 1H), 2.39 (m, 1H) ppm. ^{13}C NMR (150 MHz, Acetone-d_6): δ 162.6, 159.7, 159.6, 154.1, 145.9, 136.7, 136.6, 135.9, 134.4, 131.0, 130.9, 128.9, 128.7, 128.6, 127.5, 126.6, 126.5, 126.0, 114.1, 114.0, 89.16, 88.0, 87.5, 71.6, 64.3, 55,47, 55.44, 42.9 ppm. HRMS (MALDI-TOF) m/z: calcd for $C_{38}H_{34}F_3N_4O_6$ 699.2430 (MH^+), found 699.2439 (MH^+).

***p*-(Trifluoromethyl)phenyl-imidazolo-(2′-deoxy-5′-*O*-dimethoxytrityl)-cytidine 3′-(2-cyanoethyl)-*N,N*-diisopropylphosphoramidite (20).** A 0.45 M solution of tetrazole (0.086 mmol, 0.200 mL) in anhydrous acetonitrile was added, with stirring under a flow of argon, to a solution of **19** (60 mg, 0.086 mmol) in anhydrous acetonitrile (0.430 mL), followed by 2-cyanoethyl *N,N,N′,N′*-tetraisopropylphosphoramidite (0.086 mmol, 28 μL). TLC analysis showed that the reaction was completed within 1 h, with the formation of two diastereoisomers. The precipitated diisopropylammonium tetrazolide was removed by filtration and the solution was diluted with anhydrous acetonitrile (0.350 mL) to give 0.1 M solution of **20**. The solution was immediately used in the phosphorylation step on the automated synthesizer, without further purification. Presence of the product was confirmed by phosphorus NMR analysis. ^{31}P NMR (80 MHz, acetone-d_6): δ 149.61, 149.34 ppm. MS (ESI) m/z: calcd for $C_{47}H_{51}F_3N_6O_7P$ 899 (MH^+), found 899 (MH^+).

Absorption Measurements. Absorption spectra of analogues **1** and **2** were determined in MeOH. The concentration of the samples was in the range of 4−5 μM. The concentrations of all single-stranded and double-stranded oligonucleotides were 3 μM in PBS buffer containing NaC1 (8.0 g), KC1 (0.2 g), Na_2HPO_4 (1.15 g), KH_2PO_4 (0.2 g), in water (100 mL, pH 7.4) at 25 °C. Samples were measured at room temperature in a 10 mm quartz cell with a 1 cm path length.

Fluorescence Measurements. Emission spectra of analogues **5a−g** were determined in MeOH. The concentration of the samples was in the range of 3−3.5 μM. The emission wavelengths of all the single-stranded and double-stranded oligonucleotides were measured in PBS buffer (pH 7.4) at the concentration of 3 μM. All the measurement included 750 V sensitivity and a 5 nm slit and were performed at room temperature, λ_{ex} 350, λ_{em} 355−650 nm range. Samples were measured in a 10 mm quartz cell with a 1 cm path length. The fluorescence quantum yield (Φ) was determined relative to quinine sulfate in 0.1 M H_2SO_4 (λ_{ex} 350 nm, λ_{em} 446 nm, Φ 0.54).[49]

Oligonucleotide Synthesis, Workup, and Purification. The oligonucleotides were assembled using a DNA/RNA synthesizer and by the phosphoramidite method. CPGs (3 μmol, pore size 500 Å), DNA reagents, and commercially available phosphoramidite monomers were used. The synthesized, *p*-CF_3-^{Ph}ImdC-modified nucleoside phosphoramidite, **20**, was used at 0.1 M in dry acetonitrile. The oligonucleotides were cleaved from the solid support with 1:1 (v/v) 33% NH_4OH and 33% methylamine in ethanol at 65 °C, for 10 min. The crude product was purified by RP-HPLC on C-18 column and eluted with a solvent mixture of 0.1 M TEAA (pH 7), and a linear gradient over 30 min from 5% to 40% acetonitrile at a flow rate of 3

dx.doi.org/10.1021/jo5011944 | J. Org. Chem. 2014, 79, 7051−7062

mL/min. The oligomers were converted to the sodium salt using CM Sephadex C-25 equilibrated in NaCl and washed well with water. The identity of the oligomers was determined by MALDI-TOF mass spectroscopy: **ODN(CF_3-^{Ph}ImdC)** calcd for $C_{156}H_{171}F_3N_{66}O_{84}P_{14}Na$ [M + Na^+] 4825.73, found 4829.56. The yield of the synthesized (CF_3-^{Ph}ImdC)ODN after HPLC purification was 16% and the unmodified oligonucleotide, 20%.

Hybridization of Oligonucleotides. Solutions of labeled single-strands were mixed at room temperature with an equimolar amount of the complementary single strand oligonucleotides in PBS buffer (pH 7.4). Samples were hybridized by heating to 90 °C for 5 min and subsequently allowed to cool to room temperature over 2 h prior to measurements.

Extinction Coefficients and Concentration Determination. Extinction coefficients of the compounds were determined in MeOH. Concentrations of oligonucleotides were calculated using the following extinction coefficients (OD260/μmol): The individual extinction coefficients at 260 nm used were ε_{dT} = 8400 M^{-1} cm^{-1}, ε_{dC} = 7050 M^{-1} cm^{-1}, ε_{dG} = 12 010 M^{-1} cm^{-1}, ε_{dA} = 15 200 M^{-1} cm^{-1}, ε_G= 11500 M^{-1} cm^{-1}, ε_A= 15400 M^{-1} cm^{-1}, ε_U = 9900 M^{-1} cm^{-1}, ε_C = 7200 M^{-1} cm^{-1} and $\varepsilon_{CF3\text{-}^{Ph}ImdC}$ = 13 700 M^{-1} cm^{-1}. The extinction coefficients for the modified oligonucleotides were approximated by the linear combination of the extinction coefficients of the natural nucleotides and the extinction coefficient of the modified nucleoside. To account the base stacking interactions, this linear combination was multiplied by 0.9 to give the final extinction coefficients for the oligomers. The extinction coefficients of the duplexes (ε_D) are less than the sum of the extinction coefficients of their complementary strands (ε_{S1}, ε_{S2}) due to hyprochromic effect that should be taken into account.[68] Therefore, the extinction coefficients were calculated by the following equation

$$\varepsilon_D = (1 - h_{260nm})(\varepsilon_{S1} + \varepsilon_{S2})$$

$$h_{260nm} = 0.287 f_{AT} + 0.059 f_{GC}$$

where f_{AT} and f_{GC} are the fractions of the AT and GC base pairs, respectively.

Thermal Denaturation Measurements (T_m). The T_m values of duplexes were measured in PBS buffer (pH 7.4) at 1 μM concentration. The absorbance of the samples was monitored at 260 nm and the temperature ranged from 20 to 85 °C with heating rate of 1 °C/min.

DFT Calculations. To model the absorption spectra of the ^{Ph}ImdC analogues we performed time-dependent density functional theory (TD-DFT) calculations.[69] The M06-2X functional[70] was employed, as it has been shown to provide excellent agreement with experimental spectra.[71] We note that this global functional is most appropriate for valence and Rydberg excitations, while somewhat less so for charge transfer processes.[72] All calculations were performed using the polarizable continuum model solvent description modeling MeOH.[73] The TD-DFT calculations were performed using a 6-31+G(d,p) basis set for geometry optimizations of the ground states, while for single point calculations we used the 6-311++G(3df,2p) basis set.[74] Electronic excitation spectra were calculated at the ground-state-optimized geometry corresponding to the absorption spectra. In addition to the absorption wavelengths, oscillator strengths were computed to provide information regarding the intensity of the electronic transitions. All calculations used the Gaussian 09 program.[75,75]

■ ASSOCIATED CONTENT

Supporting Information

Stern–Volmer plot of the titration of **5d** with NMPs, melting curves of ODNs, theoretical data for **21a–e** and their tautomers, and NMR spectra of compounds **5e–g**, **6**, **7**, **10e–g**, **13**, and **15–20**. This material is available free of charge via the Internet at http://pubs.acs.org/.

■ AUTHOR INFORMATION

Corresponding Author

*Fax: 972-3-6354907. Tel: 972-3-5318303. E-mail: bilha.fischer@biu.ac.il.

Notes

The authors declare no competing financial interest.

■ REFERENCES

(1) Namba, K.; Osawa, A.; Ishizaka, S.; Kitamura, N.; Tanino, K. *J. Am. Chem. Soc.* **2011**, *133*, 11466.
(2) Kricka, L. J.; Fortina, P. *Clin. Chem.* **2009**, *55*, 670.
(3) Shinar, J. *Organic Light-Emitting Devices*; Springer: New York, 2004.
(4) Valeur, B. *Molecular Fluorescence: Principles and Applications*; Wiley-VCH: Weinheim, 2002.
(5) Nir, E.; Kleinermanns, K.; Grace, L.; de Vries, M. S. *J. Phys. Chem. A* **2001**, *105*, 5106.
(6) Callis, P. R. *Annu. Rev. Phys. Chem.* **1983**, *34*, 329.
(7) Daniels, M.; Hauswirth, W. *Science* **1971**, *171*, 675.
(8) Sanborn, M. E.; Connolly, B. K.; Gurunathan, K.; Levitus, M. *J. Phys. Chem.B* **2007**, *111*, 11064.
(9) Wilhelmsson, L. M.; Holmen, A.; Lincoln, P.; Nielsen, P. E.; Norden, B. *J. Am. Chem. Soc.* **2001**, *123*, 2434.
(10) Wahba, A. S.; Damha, M. J.; Hudson, R. H. E. *Nucleic Acids Symp. Ser.* **2008**, *52*, 399.
(11) Hudson, R. H. E.; Ghorbani-Choghamarani, A. *Synlett* **2007**, 870.
(12) Sinkeldam, R. W.; Wheat, A. J.; Boyaci, H.; Tor, Y. *ChemPhysChem* **2011**, *12*, 567.
(13) Dodd, D. W.; Hudson, R. H. E. *Mini-Rev. Org. Chem.* **2009**, *6*, 378.
(14) Hudson, R. H. E.; Moszynski, J. M. *Synlett* **2006**, 2997.
(15) Segal, M.; Fischer, B. *Org. Biomol. Chem.* **2012**, *10*, 1571.
(16) Wilson, J. N.; Gao, J.; Kool, E. T.; Mayer-Enthart, E.; Wagner, C.; Barbaric, J.; Wagenknecht, H.-A. *Tetrahedron* **2007**, *63*, 3434.
(17) Onidas, D.; Markovitsi, D.; Marguet, S.; Sharonov, A.; Gustavsson, T. *J. Phys. Chem. B* **2002**, *106*, 11367.
(18) Zilbershtein-Shklanovsky, L.; Weitman, M.; Major, D. T.; Fischer, B. *J. Org. Chem.* **2013**, *78*, 11999.
(19) Fox, J.; Praag, D. *J. Org. Chem.* **1961**, *26*, 526.
(20) Damaraju, V. L.; Smith, K. M.; Mowles, D.; Nowak, I.; Karpinski, E.; Young, J. D.; Robins, M. J.; Cass, C. E. *Biochem. Pharmacol.* **2011**, *81*, 82.
(21) Nowak, I.; Damaraju, V. L.; Cass, C. E.; Young, J. D.; Robins, M. J. *Collect. Czech. Chem. Commun.* **2011**, *76*, 1395.
(22) An, H.; Girardet, J.-L.; Hong, Z.; Koh, Y.-H. Cytidine analogs and methods of use; Google Patents WO 2004/080466, 2004.
(23) Liu, C. H.; Martin, C. T. *J. Mol. Biol.* **2001**, *308*, 465.
(24) Berry, D. A.; Chien, T. C.; Townsend, L. B. *Heterocycles* **2004**, *63*, 2475.
(25) Wahba, A. S.; Azizi, F.; Deleavey, G. F.; Brown, C.; Robert, F.; Carrier, M.; Kalota, A.; Gewirtz, A. M.; Pelletier, J.; Hudson, R. H. *ACS Chem. Biol.* **2011**, *6*, 912.
(26) Noé, M. S.; Ríos, A. C.; Tor, Y. *Org. Lett.* **2012**, *14*, 3150.
(27) Kovaliov, M.; Segal, M.; Fischer, B. *Tetrahedron* **2013**, *69*, 3698.
(28) McClure, D. S. *J. Chem. Phys.* **1949**, *17*, 905.
(29) Takadate, A.; Masuda, T.; Murata, C.; Isobe, A.; Shinohara, T.; Irikura, M.; Goya, S. *Anal. Sci.* **1997**, *13*, 753.
(30) Matsunaga, H.; Santa, T.; Iida, T.; Fukushima, T.; Homma, H.; Imai, K. *Analyst* **1997**, *122*, 931.
(31) Demchenko, A. P. *Trends Biotechnol.* **2005**, *23*, 456.
(32) Okamoto, A.; Tanaka, K.; Fukuta, T.; Saito, I. *ChemBioChem* **2004**, *5*, 958.
(33) Okamoto, A.; Tanaka, K.; Fukuta, T.; Saito, I. *J. Am. Chem. Soc.* **2003**, *125*, 9296.
(34) Hattori, M.; Ohki, T.; Yanase, E.; Ueno, Y. *Bioorg. Med. Chem. Lett.* **2012**, *22*, 253.

(35) Yoshida, Y.; Niwa, K.; Yamada, K.; Tokeshi, M.; Baba, Y.; Saito, Y.; Okamoto, A.; Saito, I. *Chem. Lett.* **2010**, *39*, 116.
(36) Tinsley, R. A.; Walter, N. G. *RNA* **2006**, *12*, 522.
(37) Sinkeldam, R. W.; Greco, N. J.; Tor, Y. *Chem. Rev.* **2010**, *110*, 2579.
(38) Zhang, C.-M.; Liu, C.; Christian, T.; Gamper, H.; Rozenski, J.; Pan, D.; Randolph, J. B.; Wickstrom, E.; Cooperman, B. S.; Hou, Y.-M. *RNA* **2008**, *14*, 2245.
(39) Wahba, A. S.; Esmaeili, A.; Damha, M. J.; Hudson, R. H. *Nucleic Acids Res.* **2009**, 1048.
(40) Greco, N. J.; Sinkeldam, R. W.; Tor, Y. *Org. Lett.* **2009**, *11*, 1115.
(41) Tanpure, A. A.; Srivatsan, S. G. *Chem.—Eur. J.* **2011**, *17*, 12820.
(42) Koh, Y.-H.; Shim, J. H.; Girardet, J.-L.; Hong, Z. *Bioorg. Med. Chem. Lett.* **2007**, *17*, 5261.
(43) Fei, X. S.; Wang, J. Q.; Miller, K. D.; Sledge, G. W.; Hutchins, G. D.; Zheng, Q. H. *Nucl. Med. Biol.* **2004**, *31*, 1033.
(44) Han, X.; Ma, H.; Wang, Y. *ARKIVOC* **2007**, 150.
(45) Andresen, G.; Gundersen, L.-L.; Lundmark, M.; Rise, F.; Sundell, S. *Tetrahedron* **1995**, *51*, 3655.
(46) Mittapalli, G. K.; Osornio, Y. M.; Guerrero, M. A.; Reddy, K. R.; Krishnamurthy, R.; Eschenmoser, A. *Angew. Chem., Int. Ed.* **2007**, *46*, 2478.
(47) Evans, R. K.; Haley, B. E. *Biochemistry* **1987**, *26*, 269.
(48) Obeid, S.; Busskamp, H.; Welte, W.; Diederichs, K.; Marx, A. *Chem. Commun.* **2012**, *48*, 8320.
(49) Melhuish, W. H. *J. Phys. Chem.* **1961**, *65*, 229.
(50) Lakowicz, J. R. *Principles of Fluorescent Spectroscopy*; Springer: Baltimore, MD, 1986.
(51) McDaniel, D. S.; Brown, H. C. *J. Org. Chem.* **1958**, *23*, 420.
(52) Brown, H. C.; Okamoto, Y. *J. Am. Chem. Soc.* **1958**, *80*, 4979.
(53) Hansch, C.; Leo, A.; Taft, R. *Chem. Rev.* **1991**, *91*, 165.
(54) Cheshmedzhieva, D.; Ivanova, P.; Stoyanov, S.; Tasheva, D.; Dimitrova, M.; Ivanov, I.; Ilieva, S. *Phys. Chem. Chem. Phys.* **2011**, *13*, 18530.
(55) Sherman, W. R.; Robins, E. *Anal. Chem.* **1968**, *40*, 803.
(56) Uchiyama, S.; Santa, T.; Suzuki, S.; Yokosu, H.; Imai, K. *Anal. Chem.* **1999**, *71*, 5367.
(57) Hansch, C.; Leo, A. *Substituent Constants for Correlation Analysis in Chemistry and Biology*; Wiley: New York, 1979.
(58) Um, I.-H.; Lee, J.-Y.; Kim, H.-T.; Bae, S.-K. *J. Org. Chem.* **2004**, *69*, 2436.
(59) Seely, G. R. *J. Phys. Chem.* **1969**, *73*, 125.
(60) Motoyoshiya, J.; Fengqiang, Z.; Nishii, Y.; Aoyama, H. *Spectrochim. Acta, Part A* **2008**, *69A*, 167.
(61) Jian, C.; Seitz, W. R. *Anal. Chim. Acta* **1990**, *237*, 265.
(62) Ueno, T.; Urano, Y.; Kojima, H.; Nagano, T. *J. Am. Chem. Soc.* **2006**, *128*, 10640.
(63) Yi, S.; Men, J.; Wu, D.; Yang, M.; Sun, H.; Chen, H.; Gao, G. *Des. Monomers Polym.* **2011**, *14*, 367.
(64) Ming, X.; Seela, F. *Chem.—Eur. J.* **2012**, *18*, 9590.
(65) Okamoto, A.; Saito, Y.; Saito, I. *J. Photochem. Photobiol.* **2005**, *6*, 108.
(66) Hurley, D. J.; Seaman, S. E.; Mazura, J. C.; Tor, Y. *Org. Lett.* **2002**, *4*, 2305.
(67) Köhler, O.; Jarikote, D. V.; Seitz, O. *ChemBioChem* **2005**, *6*, 69.
(68) Tataurov, A. V.; You, Y.; Owczarzy, R. *Biophys. Chem.* **2008**, *133*, 66.
(69) Bauernschmitt, R.; Ahlrichs, R. *Chem. Phys. Lett.* **1996**, *256*, 454.
(70) Zhao, Y.; Truhlar, D. G. *Theor. Chem. Acc.* **2008**, *120*, 215.
(71) Isegawa, M.; Peverati, R.; Truhlar, D. G. *J. Chem. Phys.* **2012**, *137*, 244104.
(72) Jacquemin, D.; Perpete, E. A.; Ciofini, I.; Adamo, C.; Valero, R.; Zhao, Y.; Truhlar, D. G. *J. Chem. Theory Comput.* **2010**, *6*, 2071.
(73) Tomasi, J.; Mennucci, B.; Cammi, R. *Chem. Rev.* **2005**, *105*, 2999.
(74) Hehre, W. J. *Acc. Chem. Res.* **1976**, *9*, 399.
(75) Frisch, M. J.; Trucks, G. W.; Schlegel, H. B.; Scuseria, G. E.; Robb, M. A.; Cheeseman, J. R.; Scalmani, G.; Barone, V.; Mennucci, B.; Petersson, G. A.; Nakatsuji, H.; M.Caricato, Li, X.; Hratchian, H. P.; Izmaylov, A. F.; Bloino, J.; Zheng, G.; Sonnenberg, J. L.; Hada, M.; Ehara, M.; Toyota, K.; Fukuda, R.; Hasegawa, J.; Ishida, M.; Nakajima, T.; Honda, Y.; Kitao, O.; Nakai, H.; Vreven, T.; Montgomery, J. A., Jr.; Peralta, J. E.; Ogliaro, F.; Bearpark, M.; Heyd, J. J.; Brothers, E.; Kudin, K. N.; Staroverov, V. N.; Kobayashi, R.; Normand, J.; Raghavachari, K.; Rendell, A.; Burant, J. C.; Iyengar, S. S.; Tomasi, J.; Cossi, M.; Rega, N.; Millam, J. M.; Klene, M.; Knox, J. E.; Cross, J. B.; Bakken, V.; Adamo, C.; Jaramillo, J.; Gomperts, R.; Stratmann, R. E.; Yazyev, O.; Austin, A. J.; Cammi, R.; Pomelli, C.; Ochterski, J. W.; Martin, R. L.; Morokuma, K.; Zakrzewski, V. G.; Voth, G. A.; Salvador, P.; Dannenberg, J. J.; Dapprich, S.; Daniels, A. D.; Ö. Farkas, Foresman, J. B.; Ortiz, J. V.; Cioslowski, J.; Fox, D. J. Gaussian, Inc.: Wallingford, CT, 2009.